Computational Mechanics 30 (2003) 131–142 © Springer-Verlag 2003
DOI 10.1007/s00466-002-0373-4

Warping shear stresses in nonuniform torsion by BEM

E. J. Sapountzakis, V. G. Mokos

Abstract In this paper a boundary element method is developed for the nonuniform torsion of simply or multiply connected prismatic bars of arbitrary cross section. The bar is subjected to an arbitrarily distributed twisting moment, while its edges are restrained by the most general linear torsional boundary conditions. Since warping is prevented, beside the Saint–Venant torsional shear stresses, the warping normal and shear stresses are also computed. Three boundary value problems with respect to the variable along the beam angle of twist and to the primary and secondary warping functions are formulated and solved employing a BEM approach. Both the warping and the torsion constants using only boundary discretization together with the torsional shear stresses and the warping normal and shear stresses are computed. Numerical results are presented to illustrate the method and demonstrate its efficiency and accuracy. The magnitude of the warping shear stresses due to restrained warping is investigated by numerical examples with great practical interest.

Keywords Nonuniform torsion, Shear stresses, Warping, Bar, Beam, Twist, Boundary element method

1 Introduction

In engineering practice we often come across the analysis of members of structures subjected to twisting moments. Curved bridges, ribbed plates subjected to eccentric loading or columns laid out irregularly in the interior of a plate due to functional requirements are most common examples.

When the warping of the cross section of the member is not restrained the applied twisting moment is undertaken from the Saint–Venant shear stresses. In this case the angle of twist per unit length remains constant along the bar. However, in most cases arbitrary torsional boundary conditions are applied either at the edges or at any other interior point of the bar due to construction requirements. This bar under the action of general twisting loading is leaded to nonuniform torsion, while the angle of twist per unit length is no longer constant along it.

Although there is extended literature on the Saint–Venant torsion problem for homogeneous isotropic prismatic bars with simply or multiply connected cross sections (Haberl and Och, 1974; Marguerre, 1940; Sauer, 1980; Katsikadelis and Sapountzakis, 1985), relatively little work has been done on the corresponding problem of nonuniform torsion. Especially because of the mathematical complexity of the problem, the existing analytical solutions are limited to symmetric cross sections of simple geometry, loading and boundary conditions (Cornelius, 1951; Bornscheuer, 1952, 1953; Friemann, 1993; Ramm and Hofmann, 1995). Moreover, numerical methods such as the finite element method (Gruttmann et al., 1998; Wagner and Gruttmann, 2001) or the boundary element method (Chen et al., 1998; Friedman and Kosmatka, 2000; Sapountzakis, 2000) have also been used for the analysis of the nonuniform torsion problem, in the case the geometry of the cross section, its boundary conditions or its loading are not simple. In all the aforementioned references the analysis of the nonuniform torsion problem is not complete, since the secondary shear stresses due to warping are not evaluated.

In this paper a boundary element method is developed for the nonuniform torsion of simply or multiply connected prismatic bars of arbitrary cross section. The beam is subjected to an arbitrarily distributed twisting moment while its edges are restrained by the most general linear torsional boundary conditions. The developed method is an improvement of that presented by Sapountzakis (2000), since it accomplishes the evaluation of the secondary warping function leading to the computation of the secondary shear stresses due to warping. Moreover, the developed procedure is a pure BEM, since it requires only boundary discretization. Three boundary value problems with respect to the variable along the beam angle of twist and to the primary and secondary warping functions are formulated and solved employing a BEM approach. Numerical results are presented to illustrate the method and demonstrate its efficiency and accuracy. The magnitude of the evaluated warping shear stresses due to restrained warping necessitates the consideration of these additional shear stresses near the restrained edges.

2 Statement of the problem

Consider a prismatic bar of length l with a cross section of arbitrary shape, occupying the two dimensional multiply

Received: 13 November 2001 / Accepted: 2 October 2002

E. J. Sapountzakis (✉)
Institute of Structural Analysis and Seismic Research,
Department of Civil Engineering,
National Technical University of Athens,
Zografou Campus, GR15773

V. G. Mokos
Institute of Structural Analysis and Seismic Research,
Department of Civil Engineering,
National Technical University of Athens,
Zografou Campus, GR15773

connected region Ω of the x, y plane bounded by the $K+1$ curves $\Gamma_1, \Gamma_2, ..., \Gamma_K, \Gamma_{K+1}$ as shown in Fig. 1.

When the bar is subjected to the arbitrarily distributed twisting moment $m_t = m_t(z)$ its angle of twist is governed by the following boundary value problem (Sapountzakis, 2000)

$$EC_M \frac{\mathrm{d}^4\theta}{\mathrm{d}z^4} - GI_t \frac{\mathrm{d}^2\theta}{\mathrm{d}z^2} = m_t \quad \text{inside the beam} \tag{1}$$

$$\alpha_1\theta + \alpha_2 M_t = \alpha_3 \tag{2a}$$

at the beam ends $z = 0, l$

$$\beta_1 \frac{\mathrm{d}\theta}{\mathrm{d}z} + \beta_2 M_b = \beta_3 \tag{2b}$$

where E, G are the modulus of elasticity and the shear modulus of the material of the bar; C_M and I_t are the warping constant and the torsion constant of the beam cross section, respectively. Moreover, $\mathrm{d}\theta/\mathrm{d}z$ denotes the rate of change of the angle of twist θ and it can be regarded as the torsional curvature, while M_t is the twisting moment and M_b is the warping moment due to the torsional curvature at the boundary of the beam given as

$$M_t = M_t^P + M_t^S \tag{3a}$$

$$M_b = -EC_M \frac{\mathrm{d}^2\theta}{\mathrm{d}z^2} \tag{3b}$$

In Eq. (3a) M_t^P is the primary twisting moment resulting from primary shear stress distribution and M_t^S is the secondary twisting moment resulting from secondary shear stress distribution due to warping (Figs. 2, 3) given as

$$M_t^P = GI_t \frac{\mathrm{d}\theta}{\mathrm{d}z} \tag{4a}$$

$$M_t^S = -EC_M \frac{\mathrm{d}^3\theta}{\mathrm{d}z^3} \tag{4b}$$

Finally, α_i, $\beta_i (i = 1, 2, 3)$ are functions specified at the boundary of the beam.

The boundary conditions (2a, b) are the most general linear torsional boundary conditions for the beam problem including also the elastic support. It is apparent that all types of the conventional torsional boundary conditions (clamped, simply supported, free or guided edge) can be derived form these equations by specifying appropriately the functions α_i and β_i (e.g. for a clamped edge it is $\alpha_1 = \beta_1 = 1$, $\alpha_2 = \alpha_3 = \beta_2 = \beta_3 = 0$).

The solution of the boundary value problem given from Eqs. (1), (2a, b) which represents the nonuniform torsion of bars presumes the evaluation of the warping and torsion constants C_M and I_t, respectively, which are given as

$$C_M = \int_\Omega \varphi_M^{P^2} \,\mathrm{d}\Omega \tag{5a}$$

$$I_t = \int_\Omega \left(x^2 + y^2 + x\frac{\partial \varphi_M^P}{\partial y} - y\frac{\partial \varphi_M^P}{\partial x} \right) \mathrm{d}\Omega \tag{5b}$$

where $\varphi_M^P(x, y)$ is the primary warping function with respect to the shear center M of the cross section of the bar, which can be established by solving independently the Neumann problem

$$\nabla^2 \varphi_M^P = 0 \quad \text{in } \Omega \tag{6}$$

$$\frac{\partial \phi_M^P}{\partial n} = y n_x - x n_y \quad \text{on } \Gamma \tag{7}$$

where $\nabla^2 = \partial^2/\partial x^2 + \partial^2/\partial y^2$ is the Laplace operator; $\partial/\partial n$ denotes the directional derivative normal to the boundary Γ and n_x, n_y the direction cosines.

It is worth noting that in the case the origin O of the coordinates is a point of the $\bar{x}, \bar{y}$ plane other than the shear center, the warping function with respect to this point φ_O^P is first established from the Neumann problem (6), (7) substituting φ_M^P by φ_O^P. Using the evaluated warping function φ_O^P, φ_M^P is then established using the transformation given by the following equation (Marguerre, 1940)

$$\varphi_M^P(x, y) = \varphi_O(\bar{x}, \bar{y}) - \overline{xy}_M + \overline{yx}_M + c^P \tag{8}$$

where $x = \bar{x} - \bar{x}_M$, $y = \bar{y} - \bar{y}_M$, $\bar{x}_M, \bar{y}_M$ are the coordinates of the shear center M with respect to $O\overline{xy}$ system of coordinates (see Fig. 1) and c^P an integration constant. The latter are given from the solution of the following linear system of equations (Sapountzakis, 2000)

$$I_{\bar{x}}\bar{x}_M + I_{\overline{xy}}\bar{y}_M + S_{\bar{x}}c^P = -R_{\bar{x}} \tag{9a}$$

$$I_{\overline{xy}}\bar{x}_M + I_{\bar{y}}\bar{y}_M - S_{\bar{y}}c^P = R_{\bar{y}} \tag{9b}$$

$$S_{\bar{x}}\bar{x}_M - S_{\bar{y}}\bar{y}_M + Ac^P = -R_{\bar{s}} \tag{9c}$$

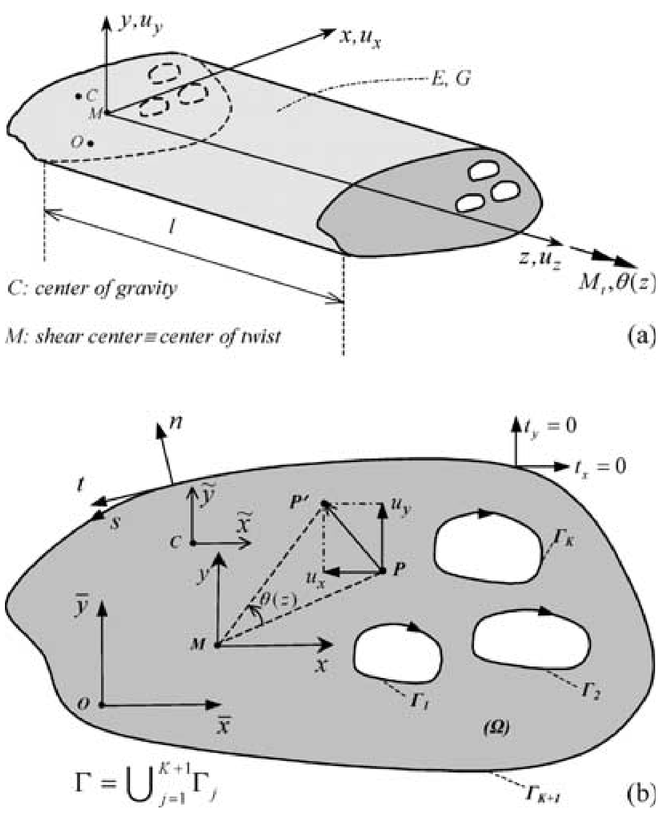

Fig. 1. Prismatic bar subjected to a twisting moment **a** with a cross section of arbitrary shape occupying the two dimensional region Ω **b**

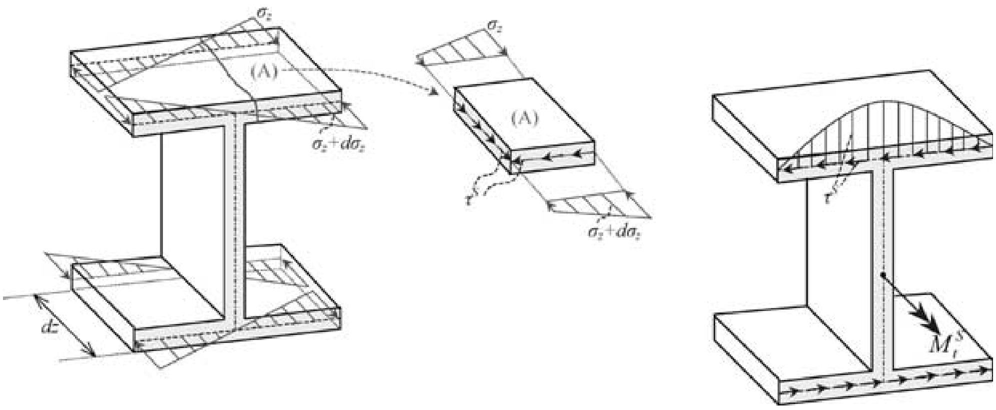

Fig. 2. Normal and shear stresses due to warping

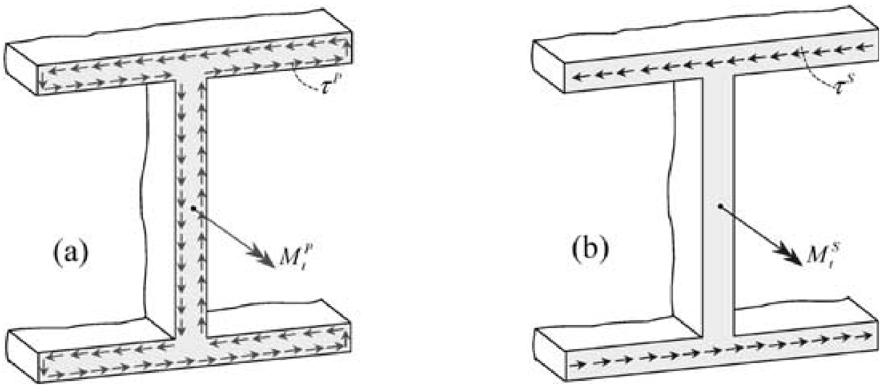

Fig. 3. Primary **a** and secondary **b** shear stress distributions

where $I_{\bar{x}}, I_{\bar{y}}$ are the moments of inertia of the cross section with respect to $\bar{x}$ and $\bar{y}$ axes, respectively; $I_{\overline{xy}}$ is its product of inertia; $S_{\bar{x}}, S_{\bar{y}}$ are the static moments of inertia of the cross section; A is its area; $R_{\bar{x}}, R_{\bar{y}}$ and $R_{\bar{s}}$ are the warping moments with respect to $\bar{x}$ and $\bar{y}$ axes and the static warping moment, respectively, given by the following equations (Sapountzakis, 2000)

$$R_{\bar{x}} = \int_{\Omega} \bar{y}\varphi_O^P \, \mathrm{d}\Omega \tag{10a}$$

$$R_{\bar{y}} = \int_{\Omega} \bar{x}\varphi_O^P \, \mathrm{d}\Omega \tag{10b}$$

$$R_{\bar{s}} = \int_{\Omega} \varphi_O^P \, \mathrm{d}\Omega \tag{10c}$$

Moreover, the basic secondary warping function $\bar{\varphi}_M^S$ is established by solving the Neumann problem

$$\nabla^2 \bar{\varphi}_M^S = -\frac{E}{G}\frac{\mathrm{d}^3\theta}{\mathrm{d}z^3}\varphi_M^P \quad \text{in } \Omega \tag{11}$$

$$\frac{\partial \bar{\varphi}_M^S}{\partial n} = 0 \quad \text{on } \Gamma \tag{12}$$

It is worth noting that the evaluated warping function $\bar{\varphi}_M^S$ due to the solution of the Neumann problem contains an integration constant c^S (parallel displacement of the cross section along the beam axis), which can be obtained from (Mokos, 2001)

$$c^S = -\frac{1}{A}\int_{\Omega} \bar{\varphi}_M^S \, \mathrm{d}\Omega \tag{13}$$

and the main secondary warping function φ_M^S is given as

$$\varphi_M^S = \bar{\varphi}_M^S + c^S \tag{14}$$

Finally, the displacement components in the x, y and z directions are evaluated from the established angle of twist θ using the relations

$$u_x = -y\theta(z) \tag{15a}$$

$$u_y = x\theta(z) \tag{15b}$$

$$u_z = \frac{\mathrm{d}\theta}{\mathrm{d}z}\varphi_M^P(x, y) \tag{15c}$$

while the nonzero stress components in the region Ω are obtained applying the theory of elasticity in terms of both the primary φ_M^P and the secondary φ_M^S warping functions as

$$\sigma_z = E\frac{\mathrm{d}^2\theta}{\mathrm{d}z^2}\varphi_M^P(x, y) \tag{16a}$$

$$\tau_{zx} = \tau_{zx}^P + \tau_{zx}^S = G\frac{\mathrm{d}\theta}{\mathrm{d}z}\left(\frac{\partial \varphi_M^P}{\partial x} - y\right) + G\frac{\partial \varphi_M^S}{\partial x} \tag{16b}$$

$$\tau_{zy} = \tau_{zy}^P + \tau_{zy}^S = G\frac{\mathrm{d}\theta}{\mathrm{d}z}\left(\frac{\partial \varphi_M^P}{\partial y} - x\right) + G\frac{\partial \varphi_M^S}{\partial y} \tag{16c}$$

3
Integral representations – numerical solution

3.1
For the angle of twist θ

The evaluation of the angle of twist θ is accomplished using BEM as this is presented in Sapountzakis (2000).

3.2
For the primary warping function φ_M^P

The integral representations and the numerical solution for the angle of twist θ assume that the warping and the torsion constants C_M and I_t, respectively, given from Eqs. (5a, b) are already established. Equations (5a, b) indicate that the evaluation of the aforementioned constants presumes that both the primary warping function φ_M^P and its derivatives with respect to x and y at any interior point of the domain Ω of the cross section of the beam are known. Once $\varphi_M^P, \partial\varphi_M^P/\partial x, \partial\varphi_M^P/\partial y$ are established C_M and I_t constants are evaluated by converting the domain integrals into line integrals along the boundary using the following relations

$$C_M = -\int_\Gamma B\frac{\partial\varphi_M^P}{\partial n}\,\mathrm{d}s \tag{17a}$$

$$I_t = \int_\Gamma \left[\left(xy^2 - y\varphi_M^P\right)n_x + \left(x^2y + x\varphi_M^P\right)n_y\right]\mathrm{d}s \tag{17b}$$

and using constant boundary elements for the approximation of these line integrals. In Eqs. (17a, b) B is a fictitious function defined as the solution of the Neumann problem

$$\nabla^2 B = \varphi_M^P \quad \text{in } \Omega \tag{18a}$$

$$\frac{\partial B}{\partial n} = 0 \quad \text{on } \Gamma \tag{18b}$$

where $\Gamma = \cup_{j=1}^{K+1}\Gamma_j$ for the case of a multiply connected region.

Moreover, Eq. (8) can give the primary warping function φ_M^P with respect to the shear center M if the warping function φ_O^P with respect to the origin of the coordinates is first established. The evaluation of the warping function φ_O^P is accomplished using BEM as this is presented in Sapountzakis (2000).

Once the warping function φ_O^P at any point inside the domain Ω is established the warping function φ_M^P with respect to the shear center M is evaluated using relations (8) and (9), after converting the domain integrals into line integrals along the boundary using the following relations

$$A = \frac{1}{2}\int_\Gamma \left(\bar{x}n_{\bar{x}} + \bar{y}n_{\bar{y}}\right)\mathrm{d}s \quad S_{\bar{x}} = \int_\Gamma \overline{xy}n_{\bar{x}}\,\mathrm{d}s$$

$$S_{\bar{y}} = \int_\Gamma \overline{xy}n_{\bar{y}}\,\mathrm{d}s \tag{19a, b, c}$$

$$I_{\bar{x}} = \int_\Gamma \overline{xy}^2 n_{\bar{x}}\mathrm{d}s \quad I_{\bar{y}} = \int_\Gamma \bar{x}^2\bar{y}n_{\bar{y}}\,\mathrm{d}s$$

$$I_{\overline{xy}} = -\frac{1}{4}\int_\Gamma \overline{xy}\left(\bar{x}n_{\bar{x}} + \bar{y}n_{\bar{y}}\right)\mathrm{d}s \tag{19d, e, f}$$

$$R_{\bar{x}}^P = \frac{1}{6}\int_\Gamma \bar{y}^2\left[3n_{\bar{y}}\phi_O^P - \bar{y}\left(\bar{y}n_{\bar{x}} - \bar{x}n_{\bar{y}}\right)\right]\mathrm{d}s \tag{19g}$$

$$R_{\bar{y}}^P = \frac{1}{6}\int_\Gamma \bar{x}^2\left[3n_{\bar{x}}\phi_O^P - \bar{x}\left(\bar{y}n_{\bar{x}} - \bar{x}n_{\bar{y}}\right)\right]\mathrm{d}s \tag{19h}$$

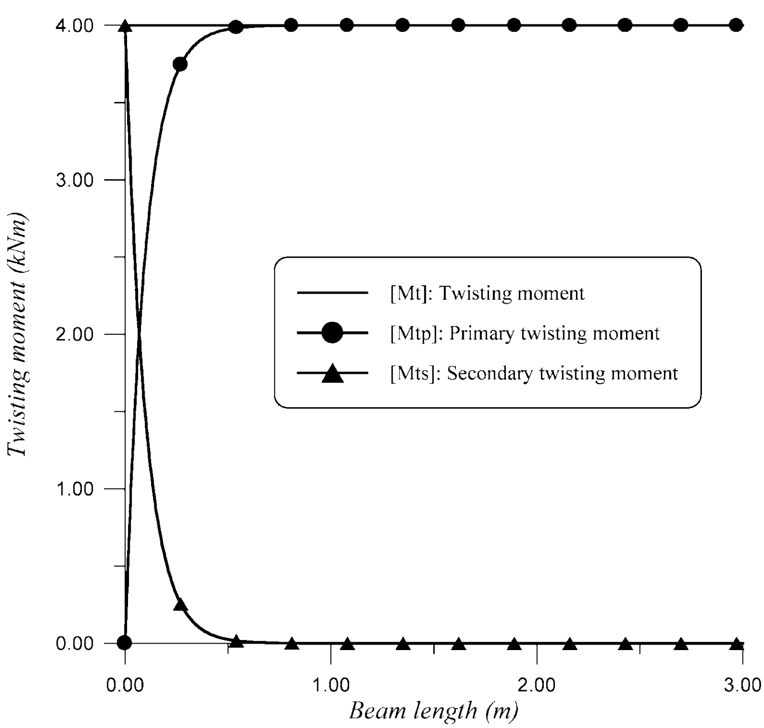

Fig. 4. Primary M_t^P, secondary M_t^S and total M_t twisting moments along the beam

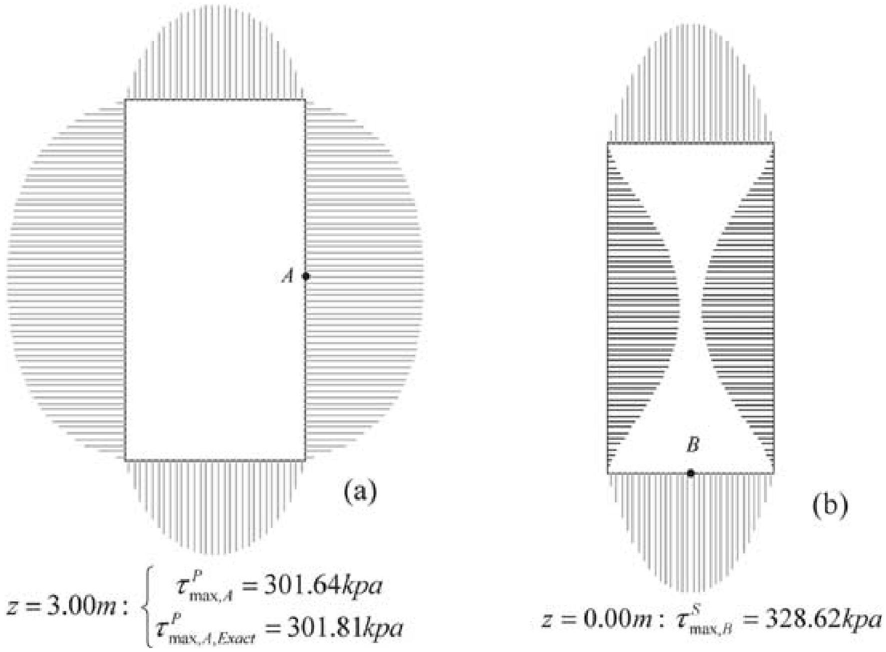

Fig. 5. Distributions of the primary **a** and the secondary **b** shear stress components along the boundary of the rectangular cross section

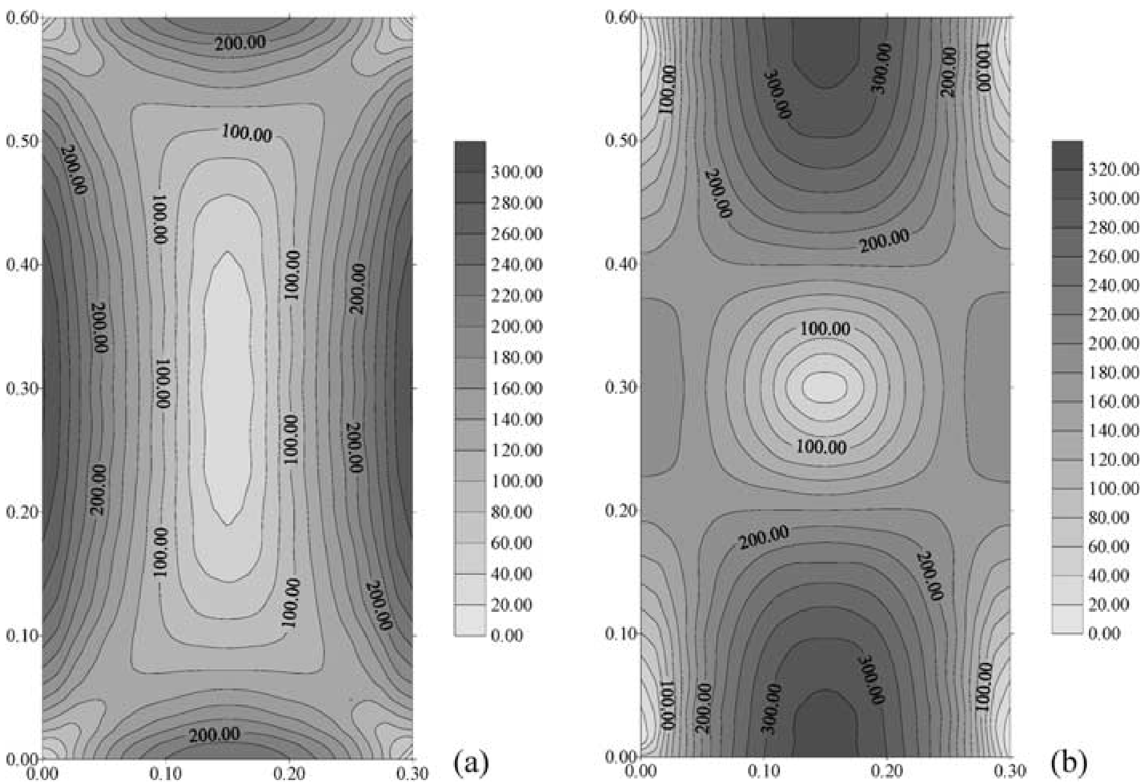

Fig. 6. Distributions of the primary **a** and the secondary **b** shear stress components in the interior of the rectangular cross section

$$R^{P}_{\bar{s}} = \frac{1}{4}\int_{\Gamma} \left[2\phi^{P}_{O}\left(n_{\bar{x}}\bar{x} + n_{\bar{y}}\bar{y}\right) - \left(\bar{x}^2 + \bar{y}^2\right)\left(\bar{y}n_{\bar{x}} - \bar{x}n_{\bar{y}}\right)\right] \mathrm{d}s \tag{19i}$$

Finally, the derivatives of φ^{P}_{M} with respect to x and y at any interior point for the calculation of the stress resultants (Eqs. 16) are computed following the procedure presented in Sapountzakis (2000).

3.3 For the secondary warping function φ^{S}_{M}

Similarly with the primary warping function, for the evaluation of the main secondary warping function φ^{S}_{M} the Green identity

$$\int_{\Omega} \left(\Psi\nabla^2\varphi - \varphi\nabla^2\Psi\right) \mathrm{d}\Omega = \int_{\Gamma} \left(\Psi\frac{\partial\varphi}{\partial n} - \varphi\frac{\partial\Psi}{\partial n}\right) \mathrm{d}s \tag{20}$$

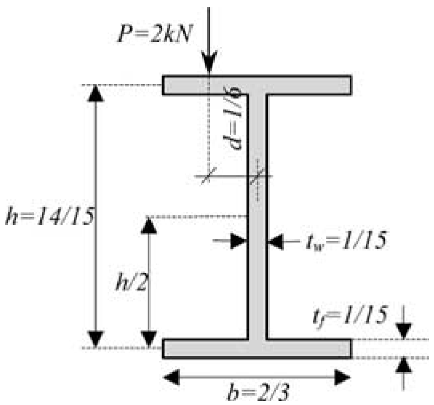

Fig. 7. Steel-I cross section

when applied to the basic secondary warping function $\bar{\varphi}_M^S$ and to the fundamental solution Ψ given by

$$\Psi = \frac{1}{2\pi} \ln r(P,Q), \quad r = |P - Q|, \qquad P, Q \in \Omega \tag{21}$$

which is a particular singular solution of the equation

$$\nabla^2 \Psi = \delta(P,Q) \tag{22}$$

yields

$$\varepsilon \bar{\varphi}_M^S(P) = \int_\Omega \ln r \nabla^2 \bar{\varphi}_M^S \, d\Omega + \int_\Gamma \left(\bar{\varphi}_M^S(q) \frac{\cos\alpha}{r} - \frac{\partial \bar{\varphi}_M^S(q)}{\partial n} \ln r \right) ds \tag{23}$$

where $\varepsilon = 2\pi, \pi$ or 0 depending on whether the point P is inside the domain Ω, on the boundary Γ or outside Ω, respectively. Using Eqs. (11), (12) the integral representation (23) is written as

$$\varepsilon \bar{\varphi}_M^S(P) = -\frac{E}{G} \frac{d^3\theta}{dz^3} \int_\Omega \ln r \varphi_M^P \, d\Omega + \int_\Gamma \left(\bar{\varphi}_M^S(q) \frac{\cos\alpha}{r} \right) ds \tag{24}$$

Applying once more the Green identity given by Eq. (20), for the primary warping function φ_M^P satisfying Eq. (6) and for the function U defined as

$$U = \frac{1}{8\pi} r^2 (\ln r - 1) \tag{25}$$

satisfying the following equation

$$\nabla^2 U = \Psi \tag{26}$$

the domain integral of Eq. (24) can be converted into a line integral along the boundary of the cross section and the integral representation (24) is written as

$$\varepsilon \bar{\varphi}_M^S(P) = -\frac{E}{4G} \frac{d^3\theta}{dz^3} \int_\Gamma \left(\varphi_M^P(q)(2 \ln r - 1) r \cos\alpha - \frac{\partial \varphi_M^P(q)}{\partial n} (\ln r - 1) r^2 \right) ds + \int_\Gamma \bar{\varphi}_M^S(q) \frac{\cos\alpha}{r} ds \tag{27}$$

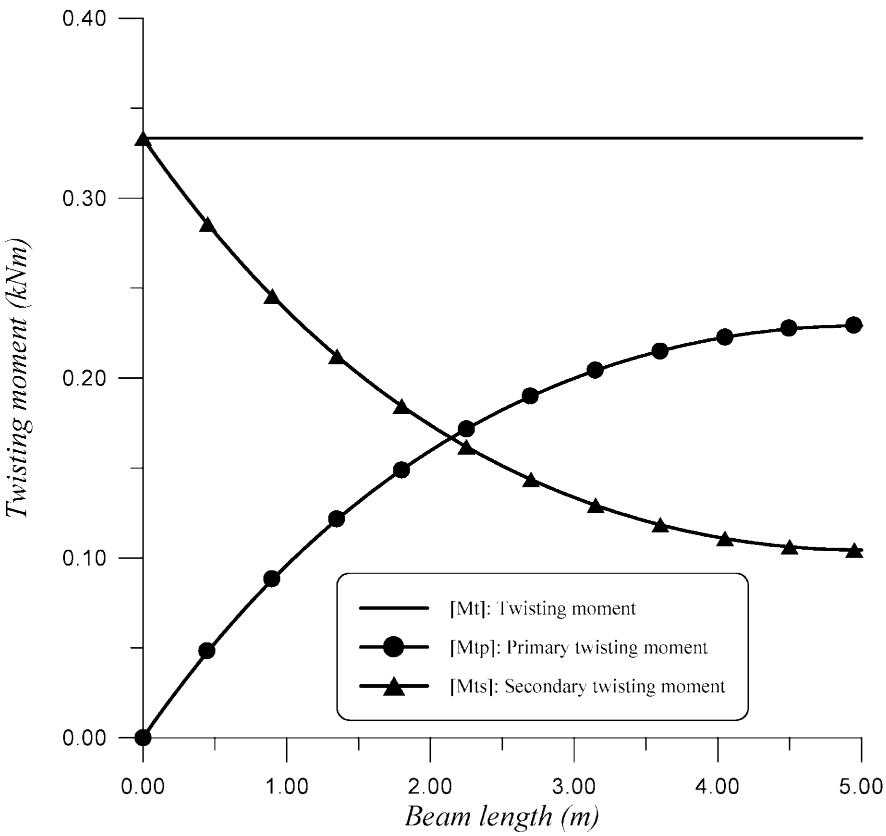

Fig. 8. Primary M_t^P, secondary M_t^S and total M_t twisting moments along the beam

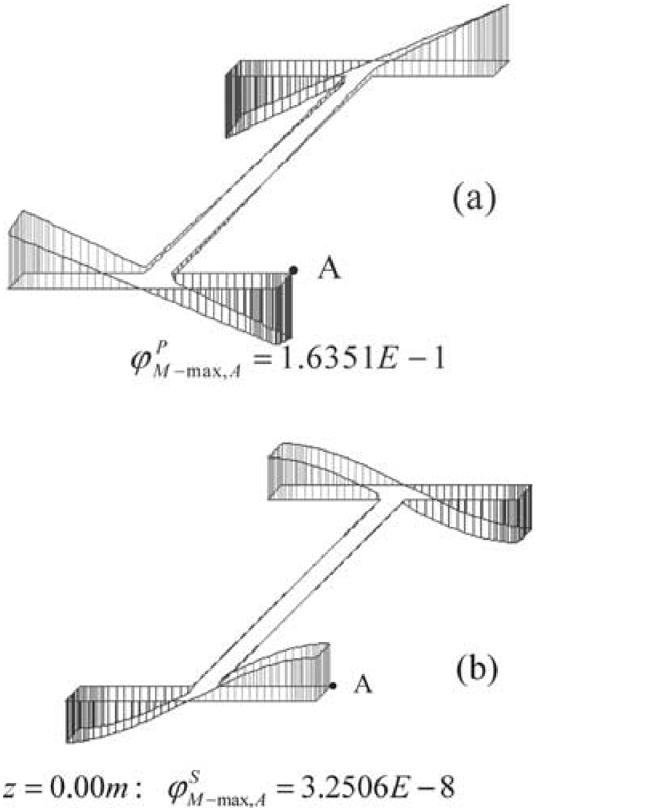

Fig. 9. Primary **a** φ^P_M and secondary **b** φ^S_M warping functions of the I cross section

The values of the function $\bar{\varphi}^S_M$ inside the domain Ω can be established from the integral representation (27) if $\bar{\varphi}^S_M$ is known on the boundary Γ. Equation (27) written for the boundary points of the domain Ω

$$\pi\bar{\varphi}^S_M(p) = -\frac{E}{4G}\frac{\mathrm{d}^3\theta}{\mathrm{d}z^3}\int_\Gamma \left(\varphi^P_M(q)(2\ln r - 1)r\cos\alpha - \frac{\partial\varphi^P_M(q)}{\partial n}(\ln r - 1)r^2\right)\mathrm{d}s + \int_\Gamma \bar{\varphi}^S_M(q)\frac{\cos\alpha}{r}\mathrm{d}s \tag{28}$$

where $r = |p - q|$, $p, q \in \Gamma$ constitutes a system of simultaneous linear equations which can be solved with respect to the unknown boundary quantities $\bar{\varphi}^S_M$. Thus, using constant boundary elements to approximate the line integrals along the boundary and a collocation technique the following linear system of simultaneous algebraic equations is established

$$\left[H^S\right]\left\{\Phi^S\right\} = \left\{F^S\right\} \tag{29}$$

where

$$\left\{\Phi^S\right\}^{\mathrm{T}} = \left\{\left(\varphi^S_M\right)_1 \quad \left(\varphi^S_M\right)_2 \quad \cdots \quad \left(\varphi^S_M\right)_N\right\} \tag{30}$$

are the values of the boundary quantities $\bar{\varphi}^S_M$ at the nodal points of the N boundary elements. Moreover, in Eq. (44) $[H^S]$ and $\{F^S\}$ are square $N \times N$ and column $N \times 1$ known coefficient matrices, respectively.

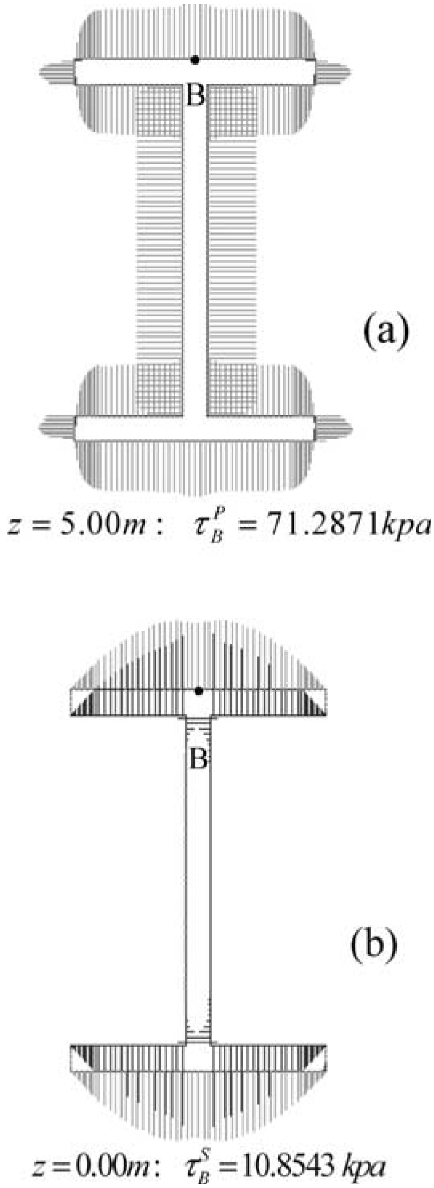

Fig. 10. Distributions of the primary **a** and the secondary **b** shear stress components along the boundary of the I cross section

Table 1. Torsion I_t and warping C_M constants and maximum value of the primary warping function φ^P_M of the I cross section of Example 2

	Thin tubes theory	BEM
Torsion constant: I_t (m^4)	$\frac{2bt_f^3 + ht_w^3}{3} = 2.2387E\text{-}4$	2.4726E-4
Warping constant: C_M (m^6)	$\frac{t_f b^3 h^2}{24} = 7.1696E\text{-}4$	7.1251E-4
Maximum value of the primary warping function: max φ^P_M (m^2)	$\frac{bh}{4} = 1.5556E\text{-}1$	1.6351E-1

Once the basic secondary warping function $\bar{\varphi}^S_M$ at any point inside the domain Ω is established the main secondary warping function φ^S_M is evaluated using relations

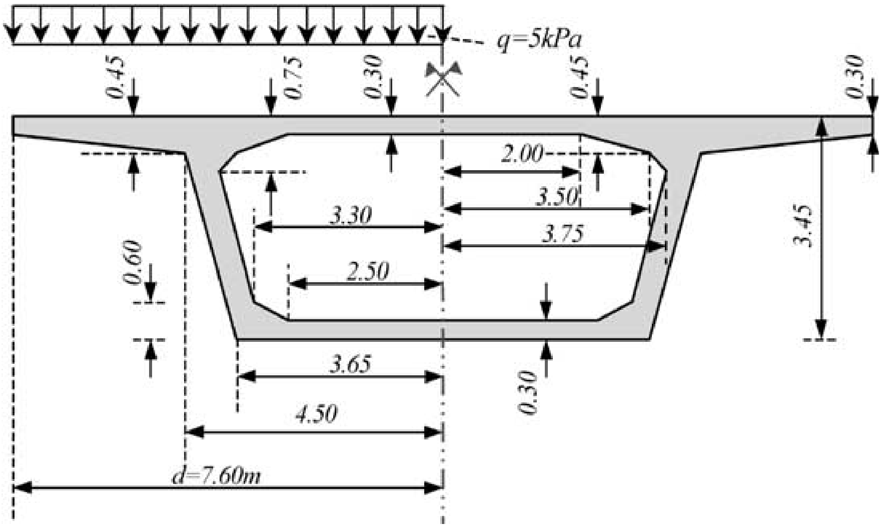

Fig. 11. Box shaped cross section

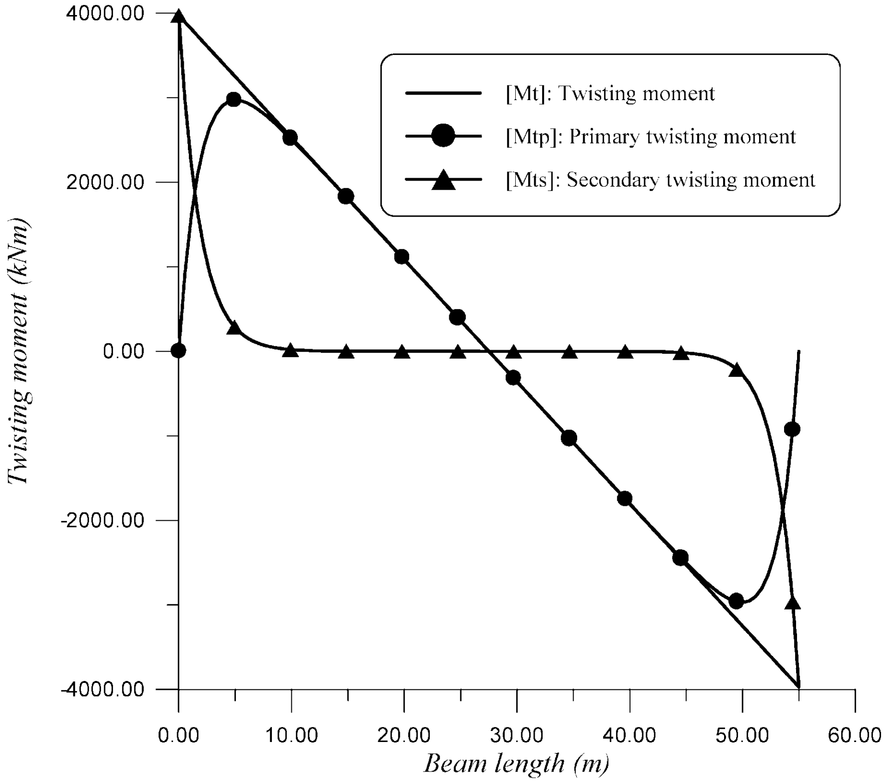

Fig. 12. Primary M_t^P, secondary M_t^S and total M_t twisting moments along the beam

(13) and (14) after converting the domain integral into line integral along the boundary using the following relation

$$\int_\Omega \bar{\varphi}_M^S \, \mathrm{d}\Omega = \frac{1}{4}\int_\Gamma \left[2\bar{\varphi}_M^S\left(n_x x + n_y y\right) - \left(x^2 + y^2\right)\left(y n_x - x n_y\right)\right] \mathrm{d}s \qquad (31)$$

Finally, the derivatives of φ_M^S with respect to x and y at any interior point for the calculation of the stress resultants (Eqs. 16) are computed differentiating the integral representation of the function φ_M^S as

$$\frac{\partial \varphi_M^S(P)}{\partial x} = \frac{E}{8\pi G}\frac{\mathrm{d}^3\theta}{\mathrm{d}z^3}\int_\Gamma \left(\varphi_M^P(q)(2\cos\omega\ \sin\alpha - (2\ln r - 1)n_x) - \frac{\partial \varphi_M^P(q)}{\partial n}(2\ln r - 1)r\cos\omega\right)\mathrm{d}s + \frac{1}{2\pi}\int_\Gamma \varphi_M^S(q)\frac{\cos(\omega - \alpha)}{r^2}\mathrm{d}s \qquad (32a)$$

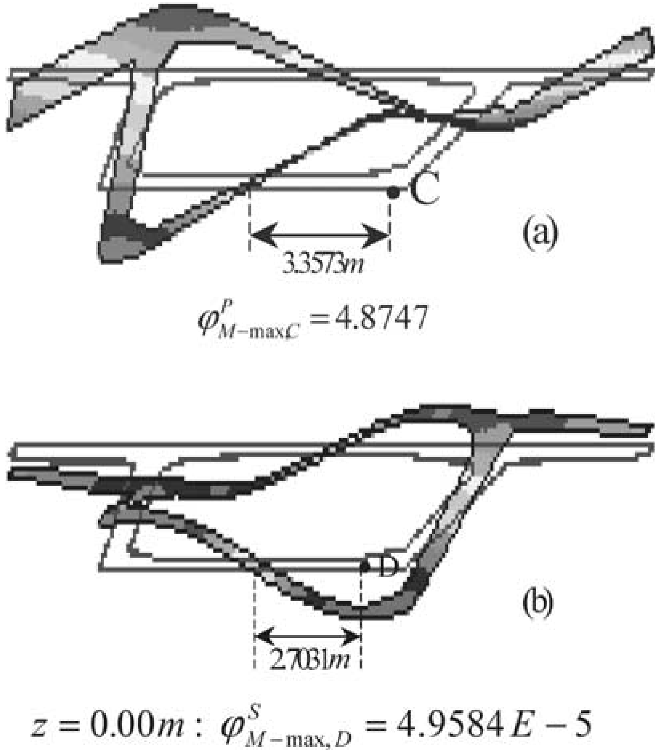

Fig. 13. Primary **a** φ_M^P and secondary **b** φ_M^S warping functions of the box shaped cross section

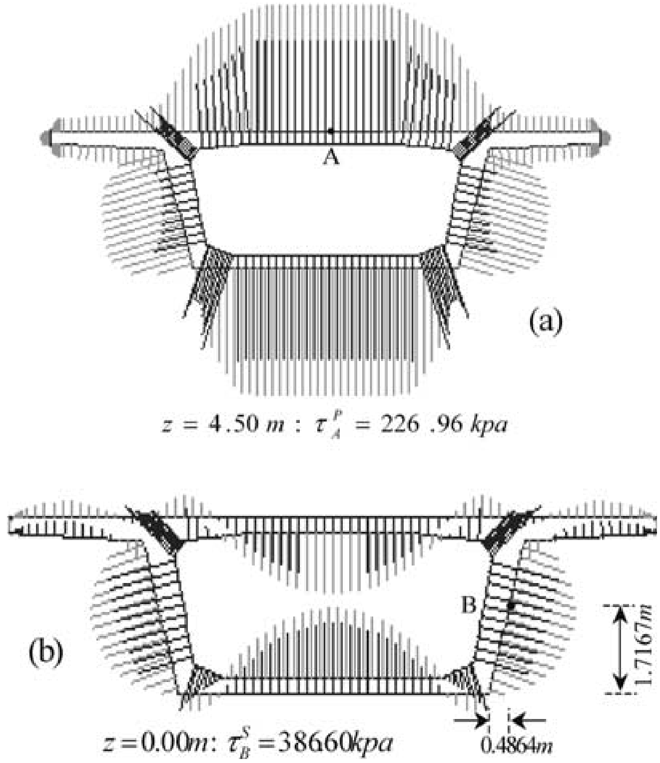

Fig. 14. Distributions of the primary **a** and the secondary **b** shear stress components along the boundary of the box shaped cross section

$$\frac{\partial \varphi_M^S(P)}{\partial y} = \frac{E}{8\pi G}\frac{d^3\theta}{dz^3}\int_\Gamma \left(\varphi_M^P(q)\big(2\sin\omega\ \sin\alpha - (2\ln r - 1)n_y\big) - \frac{\partial \varphi_M^P(q)}{\partial n}(2\ln r - 1)r\sin\omega\right)ds + \frac{1}{2\pi}\int_\Gamma \varphi_M^S(q)\frac{\sin(\omega-\alpha)}{r^2}ds \tag{32b}$$

with $\alpha = r, n$; $r = |P - q|$, $P \in \Omega$, $q \in \Gamma$ and $\omega = x, r$.

4
Numerical examples

On the basis of the analytical and numerical procedures presented in the previous sections, a computer program has been written and representative examples have been studied to demonstrate the efficiency, wherever possible the accuracy and the range of applications of the developed method. In all the examples treated the following data have been used:

Example 1
A cantilever beam of length $L = 3.0$ m, of rectangular cross section 0.30×0.60 m ($E = 3.0 \times 10^6$ kN/m^2, $\mu = 0.20$) loaded at its free end by a concentrated load $P = 2$ kN with eccentricity $d = 2.0$ m has been studied. In Fig. 4 the primary M_t^P, the secondary M_t^S and the total M_t twisting moments along the beam, while in Figs. 5, 6 the distributions of the primary and the secondary shear stress components along the boundary and in the interior of the cross section, respectively are presented. From these figures, it follows that the maximum secondary shear stress

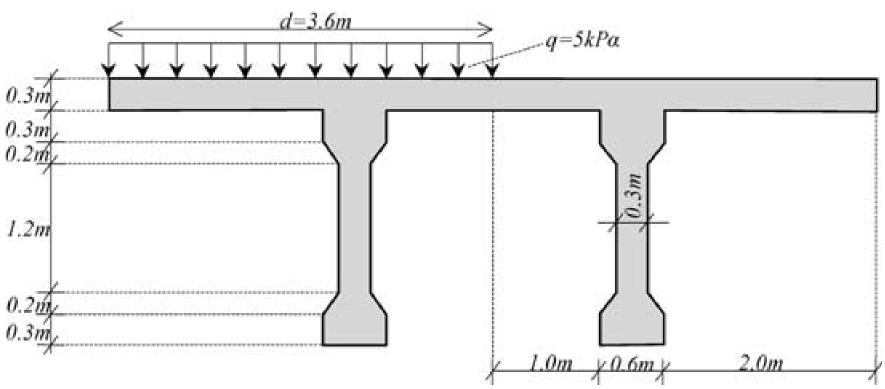

Fig. 15. Slab-and-beams cross section

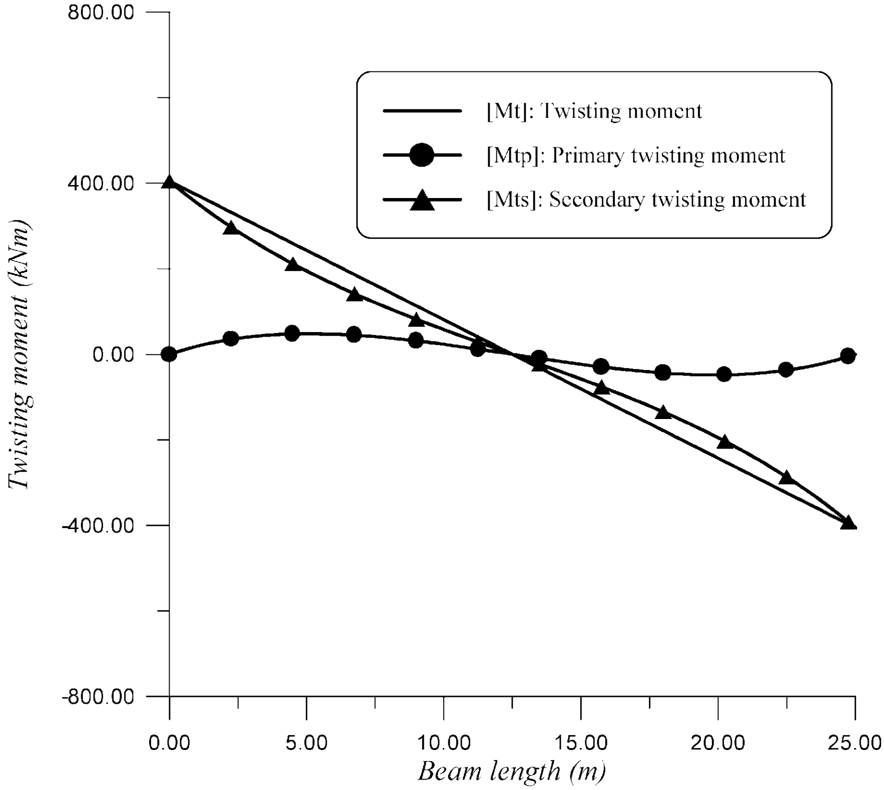

Fig. 16. Primary M_t^P, secondary M_t^S and total M_t twisting moments along the beam

due to restrained warping ($\tau_{z,\max}^S = 328.62$ kN/m^2) is of the same magnitude with the maximum primary shear stress ($\tau_{z,\max}^P = 301.64$ kN/m^2) and should not be neglected.

Example 2
A cantilever beam of length $L = 5.0$ m, of a thin-walled steel-I cross section ($E = 2.1 \times 10^8$ kN/m^2, $\mu = 0.30$) loaded at its free end by a concentrated load $P = 2$ kN with eccentricity $d = 1/6$ m has been studied (see Fig. 7). In Fig. 8 the primary M_t^P, the secondary M_t^S and the total M_t twisting moments along the beam, in Fig. 9 the primary φ_M^P and the secondary φ_M^S warping functions and in Fig. 10 the distributions of the primary and the secondary shear stress components along the boundary are presented. Moreover, in Table 1 the computed torsion I_t and warping C_M constants together with the maximum value of the primary warping function φ_M^P are shown as compared with those obtained from thin tubes theory (Timoshenko and Goodier, 1951). From both the table and the figures results the necessity of consideration of the nonuniform torsion of the beam.

Example 3
A clamped beam of length $L = 55.0$ m, of a box shaped cross section ($E = 3.0 \times 10^7$ kN/m^2, $\mu = 0.20$) eccentrically uniformly loaded, as shown in Fig. 11, has been studied. In Fig. 12 the primary M_t^P, the secondary M_t^S and

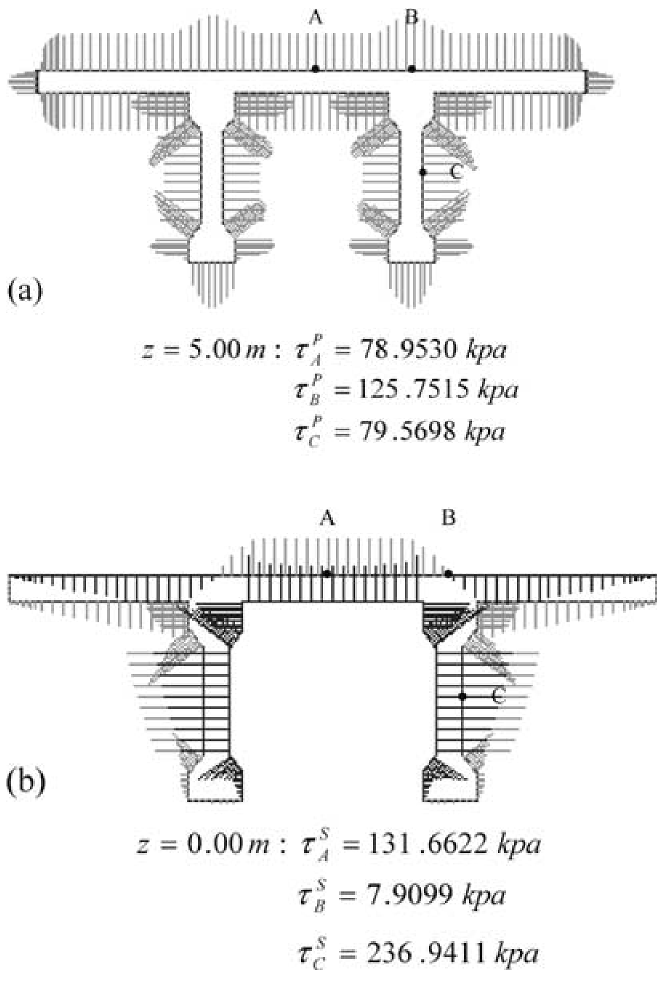

▶

Fig. 17. Distributions of the primary **a** and the secondary **b** shear stress components along the boundary of the slab-and-beams cross section

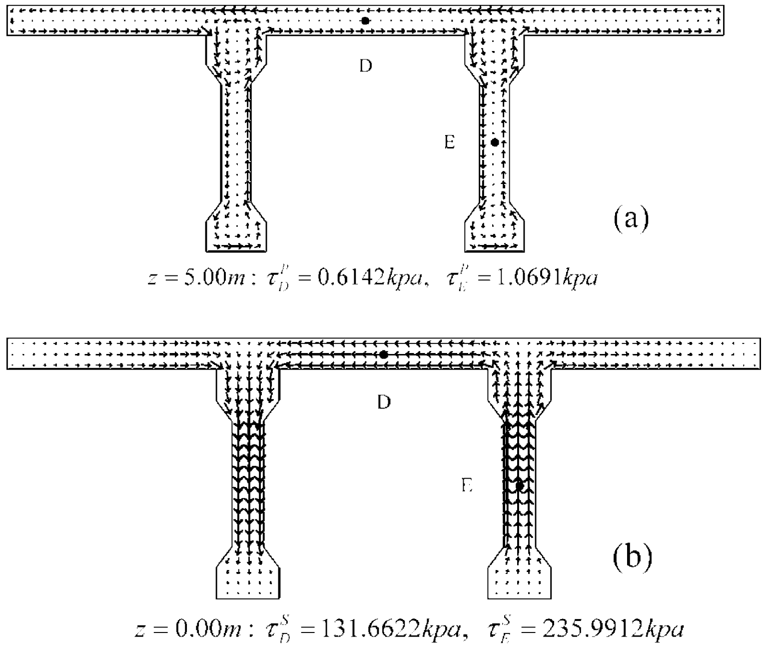

Fig. 18. Distributions of the primary **a** and the secondary **b** shear stress components in the interior of the slab-and-beams cross section

the total M_t twisting moments along the beam, in Fig. 13 the primary φ_M^P and the secondary φ_M^S warping functions, and in Fig. 14 the distributions of the primary and the secondary shear stress components along the boundary are presented. The necessity of consideration of the additional warping shear stresses near the restrained edges is once more verified.

Example 4
A clamped beam of length $L = 25.0$ m, of a slab-and-beams shaped cross section ($E = 3.0 \times 10^7$ kN/m^2, $\mu = 0.20$) eccentrically uniformly loaded, as shown in Fig. 15, has been studied. In Fig. 16 the primary M_t^P, the secondary M_t^S and the total M_t twisting moments along the beam and in Figs. 17, 18 the distributions of the primary and the secondary shear stress components along the boundary and in the interior of the cross section, respectively are presented. From these figures, it follows that the maximum secondary shear stress is greater than the maximum primary shear stress and should not be neglected.

5
Concluding remarks
In this paper a boundary element method has been developed for the nonuniform torsion of simply or multiply connected prismatic bars of arbitrary cross section. Three boundary value problems with respect to the variable along the beam angle of twist, to the primary and to the secondary warping functions are formulated and solved employing a BEM approach. Both the warping and the torsion constants together with the torsional shear stresses and the warping normal and shear stresses are computed. The main conclusions that can be drawn from this investigation are

a. The numerical technique presented in this investigation is well suited for computer aided analysis for beams of arbitrary cross section, subjected to any linear torsional boundary conditions and to an arbitrarily distributed twisting moment.
b. The magnitude of the evaluated warping shear stresses due to restrained warping necessitates the consideration of these additional shear stresses near the restrained edges.
c. The developed procedure retains the advantages of a BEM solution over a pure domain discretization method since it requires only boundary discretization.

References
Bornscheuer FW (1952) Beispiel und Formelsammlung zur Spannungsberechnung Dünnwandiger Stäbe mit Wölbbehindertem Querschnitt. Der Stahlbau 21(12): 225–232

Bornscheuer FW (1953) Beispiel und Formelsammlung zur Spannungsberechnung Dünnwandiger Stäbe mit Wölbbehindertem Querschnitt. Der Stahlbau 22(2): 32–44

Chen JT, Chen KH, Yeih W, Shieh NC (1998) Dual boundary element analysis for cracked bars under torsion. Eng. Comput. Int. J. Comp-Aided Eng. 15(6): 732–749

Cornelius W (1951) Über den Einfluss der Torsionssteifigkeit auf die Verdrehung von Tragwerken. MAN-Forschungsheft 39–65

Friedman Z, Kosmatka JB (2000) Torsion and flexure of a prismatic isotropic beam using the boundary element method. Comp. Struct. 74: 479–494

Friemann H (1993) Schub und Torsion in gerade Stäben, Werner–Verlag, Düsseldorf

Gruttmann F, Wagner W, Sauer R (1998) Zur Berechnung von Wölbfunktion und Torsionskennwerten beliebiger Stabquerschnitte mit der Methode der Finiten Elemente. Bauingenieur 73(3): 138–143

Haberl G, Och F (1974) A finite-element solution for the torsional rigidity and the shear centre of arbitrary cross section. Z. Flugwiss 22: 115–119

Kappus R (1937) Drillknicken zentrisch gedrückter Stäbe mit offenem Profil im elastischen Bereich. Luftfahrtforschung 14: 444–457

Katsikadelis JT, Sapountzakis EJ (1985) Torsion of composite bars by boundary element method. ASCE J. Eng. Mech. 111(9): 1197–1210

Marguerre K (1940) Torsion von Voll– und Hohlquerschnitten. Der Bauingenieur 21: 317–322

Mehlhorn G (1970) Ein Beitrag zum Kipp–Problem von Stahlbeton–und Spannbetonträgern, Diss. TH Darmstadt

Mehlhorn G, Schwarz P (1971) Ein Beitrag zur Bestimmung der Lage des Schubmittelpunktes. Bauingenieur 46(1): 6–10

Mokos VG (2001) Nonuniform torsion of bars by boundary element method. Postgraduate Thesis, 73, National Technical University of Athens, Civil Engineering Department

Ramm E, Hofmann TJ (1995) Der Ingenieurbau: Grundwissen – Baustatik/Baudynamik, Ernst & Sohn, Berlin

Sapountzakis EJ (2000) Solution of nonuniform torsion of bars by an integral equation method. Int. J. Comp. Struct. 77: 659–667

Sauer E (1980) Schub und Torsion bei elastischen prismatischen Balken. Mitteilungen aus dem Institut für Massivbau der Technischen Hochschule Darmstadt, 29, Verlag Wilhelm Ernst & Sohn, Berlin/München

Timoshenko S, Goodier J (1951) Theory of Elasticity, McGraw-Hill, New York

Wagner W, Gruttmann F (2001) Finite element analysis of Saint–Vernant torsion problem with exact integration of the elastic–plastic constitutive equations. Comp. Meth. Appl. Mech. Eng. 190: 3831–3848